Mathematical Analysis of Pipelines Located Through Both Liquefied and Non-Liquefied Ground

Mathematical Analysis of Pipelines Located Through Both Liquefied and Non-Liquefied Ground

Masakatsu MIYAJIMA*, Masaru KITAURA* and Tetsuo KIMURA**

Abstract

The earthquake damage data in the 1964 Niigata Earthquake and the 1983 Nipponkai-Chubu Earthquake show that the pipeline damage were found near the boundary between the liquefied and non-liquefied areas. In this paper, main factors affecting the pipe failure located through both liquefied and non-liquefied ground are considered in connection with subsidence, buoyancy and seismic motion which is different from the motion of neighboring sites. Formulae obtained by using beam theory are presented and the response characteristics of pipelines are discussed. The results suggest that serious attention should be paid to vibration-induced strains during liquefaction.

Keywords : Buried pipeline, soil liquefaction, mathematical analysis.

1. General Remarks

One of the most striking characteristics of pipeline damage during the 1983 Nipponkai-Chubu Earthquake was that all of the damage to cast iron pipe (CIP) occurred at liquefied sites and most of those occurred near the boundary between the liquefied and non-liquefied sites[1]. Fig. 1 illustrates an example of earthquake damage to a pipeline observed in the 1983 Nipponkai-Chubu Earthquake. This figure also shows failure modes of the pipelines in accordance with Fig. 2. Fig. 1 reflects that 13 failures of the cast iron pipe occurred near the boundary between the liquefied and non-liquefied sites. Damage to the pipelines seems to be induced by ground movements due to sharp change of the ground characteristics, buoyancy effect at the liquefied sites and settlement of the liquefied ground.

The purposes of the present paper are to clarify pipe behavior through a boundary between liquefied and non-liquefied sites and to discuss characteristics of the failures of the pipelines buried in such areas.

2. Mathematical Treatment

Fig. 3 shows analytical models for pipelines buried through a boundary between liquefied and non-liquefied ground. In case 1, the pipeline is assumed to be subjected to subsidence of the liquefied ground, while in case 2 buoyancy effect is a governing factor. In case 3, the pipeline is subjected to a seismic motion which is different from the motion of the neighboring zones. In this last case, the superficial layer of the ground above the liquefied layer can be regarded as a

* Department of Civil Engineering
** Graduate Student, Department of Construction and Environmental Engineering

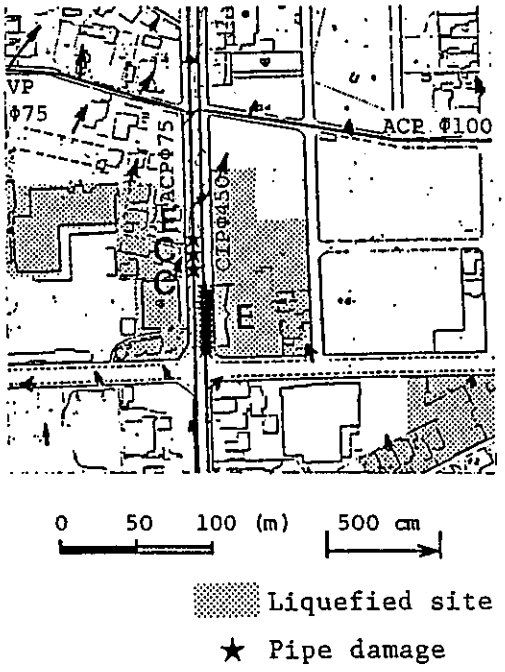

Fig. 1 Liquefied sites and pipe damage (Nagasaki in Noshiro city).

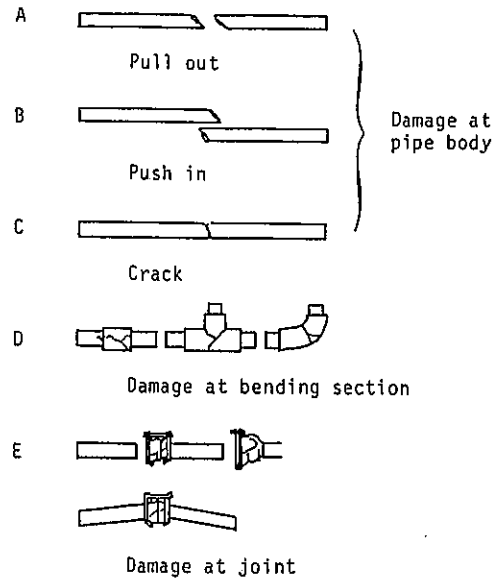

Fig. 2 Failure modes of pipeline (from Noshiro City Gas and Waterworks Bureau, 1983).

horizontally vibrating elastic plate which is subjected to a periodical driving force at both ends. These three analytical models have been constructed under the same assumptions described in Ref. 2. That is, the perfectly elastic behavior is assumed for the pipe material and the pipe motion is analyzed in the two-dimensional plane. Characteristics of the pipe strains are investigated using these simplified mathematical models. In this investigation, the responses of the pipelines can be estimated by solving the following differential equations with suitable boundary conditions.

(1) Case 1

According to the schematic representation of case 1, as shown in Fig. 3 and upon the above several assumptions, the differential equations for case 1 may be expressed as

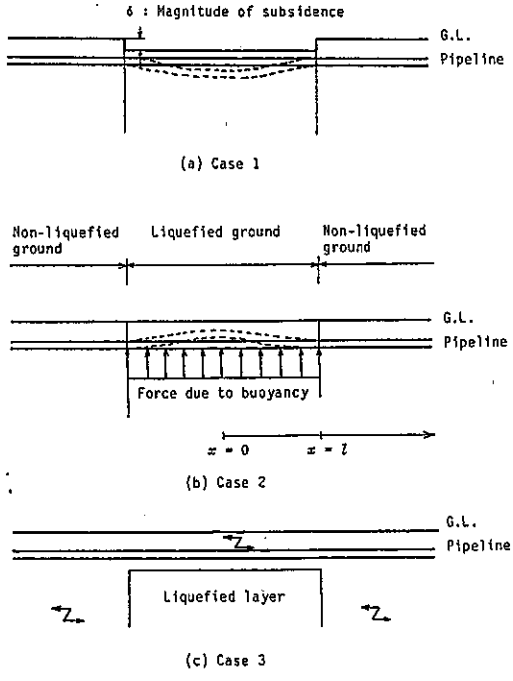

Fig. 3 Analytical models for buried pipelines located between liquefied and non-liquefied ground.

follows ;

$$EI\frac{d^4v_1}{dx^4}+K_{v_1}v_1=K_{v_1}V_1 \qquad (0<x<l) \quad (1)$$

$$EI\frac{d^4v_2}{dx^4}+K_{v_2}v_2=0 \qquad (x>l) \quad (2)$$

The boundary conditions are

$$\frac{dv_1}{dx}=0,\ \frac{d^3v_1}{dx^3}=0 \qquad (x=0) \quad (3)$$

$$v_1=v_2,\ \frac{dv_1}{dx}=\frac{dv_2}{dx},\ \frac{d^2v_1}{dx^2}=\frac{d^2v_2}{dx^2},\ \frac{d^3v_1}{dx^3}=\frac{d^3v_2}{dx^3} \qquad (x=l) \quad (4)$$

$$v_2=0,\ \frac{dv_2}{dx}=0 \qquad (x=\infty) \quad (5)$$

respectively.

(2) Case 2

Supposing that the transverse displacement in the pipeline depends on buoyancy effect, the governing differential equations for case 2 may be given by

$$EI\frac{d^4v_1}{dx^4}+K_{v_1}v_1=F \qquad (0<x<l) \quad (6)$$

$$EI\frac{d^4v_2}{dx^4}+K_{v_2}v_2=0 \qquad (x>l) \quad (7)$$

The boundary conditions Eqs. (3), (4) and (5) are also available for the problem of case 2. Therefore, Eqs. (3) through (5) are used to obtain the generalized analytical solutions of v_1 and v_2.

(3) Case 3

Since the schematic model of case 3 is taking account of the liquefaction in the superficial layer of the ground, including the original model presented by Nishio et al.[3], the differential equation can be written in a form of

$$EA\frac{d^2u_1}{dx^2}-K_{u_1}u_1=-K_{u_1}U_1 \qquad (0<x<l) \quad (8)$$

$$EA\frac{d^2u_2}{dx^2}-K_{u_2}u_2=-K_{u_2}U_2 \qquad (x>l) \quad (9)$$

The boundary conditions are

$$\frac{du_1}{dx}=0 \qquad (x=0) \quad (10)$$

$$u_1=u_2,\quad \frac{du_1}{dx}=\frac{du_2}{dx} \qquad (x=l) \qquad (11)$$

$$\frac{du_2}{dx}=0 \qquad (x=L) \qquad (12)$$

where U_1 in Eq. (8) and U_2 in Eq. (9) are expressed as follows ;

$$U_1=\frac{\cos(\frac{2\pi x}{cT})}{\cos(\frac{2\pi l}{cT})}U_{s0} \qquad (13)$$

$$U_2=U_s, \qquad (14)$$

By integrating Eqs. (1) and (2) with respect to x using the boundary conditions Eqs. (3), (4) and (5), the analytical solutions of v_1 and v_2 for case 1 are

$$v_1(x)=\exp(\beta_1 x)(A_1\cos\beta_1 x+A_2\sin\beta_1 x)+\exp(-\beta_1 x)(A_3\cos\beta_1 x+A_4\sin\beta_1 x)+\delta \qquad (0<x<l) \qquad (15)$$

$$v_2(x)=\exp(-\beta_2 x)(A_5\cos\beta_2 x+A_6\sin\beta_2 x) \qquad (x>l) \qquad (16)$$

The solution of v_1 for case 2 is

$$v_1(x)=\exp(\beta_1 x)(A_1\cos\beta_1 x+A_2\sin\beta_1 x)+\exp(-\beta_1 x)(A_3\cos\beta_1 x+A_4\sin\beta_1 x)+\frac{F}{Kv_1} \qquad (0<x<l) \qquad (17)$$

and the solution of v_2 for case 2 may be given by Eq. (16). In addition, solving Eqs. (8) and (9) with the boundary conditions Eqs. (10) through (12) gives

$$u_1(x)=A_7\cosh\lambda_1 x+\frac{U_1}{1+(\frac{2\pi}{\lambda_1 cT})^2} \qquad (0<x<l) \qquad (18)$$

$$u_2(x)=A_8\exp(\lambda_2 x)+A_9\exp(-\lambda_2 x)+U_s, \qquad (x>l) \qquad (19)$$

where A_1, $A_2\cdots$and A_9 in the above solutions are integral constants. These constants are listed in Table 1. v_0 in Table 1 is equal to δ for case 1 and F/Kv_1 for case 2, respectively.

Table 1 Integral constants.

$$A_1 = A_3 = \frac{v_0 C_1}{B_1C_1 - B_2C_2 + B_3C_3 - B_4C_4}$$

$$A_2 = -A_4 = \frac{-v_0 C_5}{-B_5C_5 + B_6C_6 - B_7C_7 + B_8C_8}$$

$$A_5 = \frac{v_0 C_9}{B_9C_9 - B_{10}C_{10} + B_{11}C_{11} - B_{12}C_{12}}$$

$$A_6 = \frac{-v_0 C_{13}}{-B_{13}C_{13} + B_{14}C_{14} - B_{15}C_{15} + B_{16}C_{16}}$$

$$A_7 = \frac{G_2}{\lambda_1 \sinh\lambda_1 l - \lambda_2 \frac{G_4}{G_3}\cosh\lambda_1 l}\left\{\frac{2}{cT}\sin G_1 - \lambda_2 \frac{G_4}{G_3}\left(\cos G_1 - \frac{U_2}{G_2}\right)\right\}$$

$$A_8 = \frac{1}{G_3}(2A_7 \cosh\lambda_1 l + G_2 \cos G_1 - U_2)$$

$$A_9 = A_8 \exp(2\lambda_2 l)$$

$$B_1 = \{\exp(\beta_1 l) + \exp(-\beta_1 l)\}\cos\beta_1 l$$
$$B_2 = D_5\{D_2\exp(\beta_1 l) - D_1\exp(-\beta_1 l)\}$$
$$B_3 = D_5^2\{-\exp(\beta_1 l) + \exp(-\beta_1 l)\}\sin\beta_1 l$$
$$B_4 = D_5^3\{-D_1\exp(\beta_1 l) + D_2\exp(-\beta_1 l)\}$$
$$B_5 = \{\exp(\beta_1 l) - \exp(-\beta_1 l)\}\sin\beta_1 l$$
$$B_6 = D_5\{D_1\exp(\beta_1 l) - D_2\exp(-\beta_1 l)\}$$
$$B_7 = D_5^2\{\exp(\beta_1 l) + \exp(-\beta_1 l)\}\cos\beta_1 l$$
$$B_8 = D_5^3\{D_2\exp(\beta_1 l) - D_1\exp(-\beta_1 l)\}$$
$$B_9 = -B_{15} = -\exp(-\beta_2 l)\cos\beta_2 l$$
$$B_{10} = -B_{16} = D_3\exp(-\beta_2 l)$$
$$B_{11} = B_{13} = -\exp(-\beta_2 l)\sin\beta_2 l$$
$$B_{12} = B_{14} = -D_4\exp(-\beta_2 l)$$

$$G_1 = \frac{2\pi l}{cT}$$

$$G_2 = \frac{U_1}{1 + \left(\frac{2\pi}{\lambda_1 cT}\right)^2}$$

$$G_3 = \exp(\lambda_2 l) + \exp\{\lambda_2(2L - l)\}$$
$$G_4 = \exp(\lambda_2 l) - \exp\{\lambda_2 L - l)\}$$

$$C_1 = B_6B_{11}B_{16} + B_{10}B_{15}B_8 + B_{14}B_{12}B_7 - B_{14}B_{11}B_8 - B_8B_{12}B_{15} - B_{10}B_7B_{16}$$
$$C_2 = B_5B_{11}B_{16} + B_9B_{15}B_8 + B_{13}B_{12}B_7 - B_{13}B_{11}B_8 - B_5B_{12}B_{15} - B_9B_7B_{16}$$
$$C_3 = B_5B_{10}B_{16} + B_9B_{14}B_8 + B_{13}B_{12}B_6 - B_{13}B_{10}B_8 - B_5B_{12}B_{14} - B_9B_6B_{16}$$
$$C_4 = B_5B_{10}B_{15} + B_9B_{14}B_7 + B_{13}B_{11}B_6 - B_{13}B_{10}B_7 - B_5B_{11}B_{14} - B_9B_8B_{15}$$
$$C_5 = B_2B_{11}B_{16} + B_{10}B_{15}B_4 + B_{14}B_{12}B_3 - B_{14}B_{11}B_4 - B_{10}B_3B_{16} - B_2B_{12}B_{15}$$
$$C_6 = B_1B_{11}B_{16} + B_9B_{15}B_4 + B_{13}B_{12}B_3 - B_{13}B_{11}B_4 - B_9B_3B_{16} - B_1B_{12}B_{15}$$
$$C_7 = B_1B_{10}B_{16} + B_9B_{14}B_4 + B_{13}B_{12}B_2 - B_{13}B_{10}B_4 - B_9B_2B_{16} - B_1B_{12}B_{14}$$
$$C_8 = B_1B_{10}B_{15} + B_9B_{14}B_3 + B_{13}B_{11}B_2 - B_{13}B_{10}B_3 - B_9B_2B_{15} - B_1B_{11}B_{14}$$
$$C_9 = B_2B_7B_{16} + B_6B_{15}B_4 + B_{14}B_8B_3 - B_{14}B_7B_4 - B_2B_8B_{15} - B_6B_3B_{16}$$
$$C_{10} = B_1B_7B_{16} + B_5B_{15}B_4 + B_{13}B_8B_3 - B_{13}B_7B_4 - B_1B_8B_{15} - B_5B_3B_{16}$$
$$C_{11} = B_1B_8B_{16} + B_5B_{14}B_4 + B_{13}B_8B_2 - B_{13}B_8B_4 - B_1B_8B_{14} - B_5B_2B_{16}$$
$$C_{12} = B_1B_6B_{15} + B_5B_{14}B_3 + B_{13}B_7B_2 - B_{13}B_6B_3 - B_1B_7B_{14} - B_5B_2B_{15}$$
$$C_{13} = B_2B_7B_{12} + B_{10}B_8B_3 + B_6B_{11}B_4 - B_{10}B_7B_4 - B_2B_8B_{11} - B_6B_3B_{12}$$
$$C_{14} = B_1B_7B_{12} + B_9B_8B_3 + B_5B_{11}B_4 - B_9B_7B_4 - B_1B_8B_{11} - B_5B_3B_{12}$$
$$C_{15} = B_1B_6B_{12} + B_9B_8B_2 + B_5B_{10}B_4 - B_9B_6B_4 - B_1B_8B_{10} - B_5B_2B_{12}$$
$$C_{16} = B_1B_6B_{11} + B_9B_7B_2 + B_5B_{10}B_3 - B_9B_6B_3 - B_1B_7B_{10} - B_5B_2B_{11}$$

$$D_1 = \cos\beta_1 l + \sin\beta_1 l$$
$$D_2 = \cos\beta_1 l - \sin\beta_1 l$$
$$D_3 = \cos\beta_2 l + \sin\beta_2 l$$
$$D_4 = \cos\beta_2 l - \sin\beta_2 l$$
$$D_5 = \frac{\beta_1}{\beta_2}$$

3. Application of Analytical Solutions to the Practical Cases

Soil spring constant shows non-linear characteristics with increasing soil displacement. However, the soil spring constant is assumed to be unchangeable irrespective of the relative displacement for simplicity in this paper. This unchangeable value is called as equivalent soil spring constant. The equivalent soil spring constant for liquefiable ground depends on the degree of liquefaction of the soil. Initially, the bending pipe stresses due to subsidence of the ground induced by liquefaction are investigated in relation to the ratio of the equivalent soil spring constant K_1/K_2 for case 1. Fig. 4 shows the relationship between : a) the maximum bending pipe stresses due to subsidence of the liquefied ground and, b) the width of the liquefaction zone. The pipelines used in this analysis are steel pipelines whose physical properties are listed in Table 2. The magnitude of subsidence of the liquefied ground is assumed to be 20cm, and it is equivalent to a 2% subsidence of 10m liquefied layer. Yoshimi et al. concluded that the average vertical strain as a result of consolidation under the weight of the soil was 1% to 3% when a horizontal layer of loose saturated sand was liquefied to a depth of approximately 5m to 20m[4]. The experimental results presented by Lee et al.[5] also agree with the results indicated by Yoshimi et al. It can be seen from Fig. 4 that the higher the ratio of the equivalent soil spring constant is, which means smaller degree of liquefaction, the greater the maximum bending pipe stresses are. It is interesting to note that the maximum bending pipe stress for each ratio of the equivalent soil spring constant does not increase in areas of liquefied ground where the width exceeds 10m. The maximum bending stress exceeds the allowable bending stress of steel pipe (4,200kgf/cm²) when the ratio of the equivalent soil spring constant is greater than 0.1, particularly at a width of liquefied zone less than 5m except for the region near 0m. Fig. 5 shows the relationship between the displacement of the pipe and the width of the liquefied zone. It can be seen from this figure that for relatively narrow width of the liquefied ground or low ratio of the

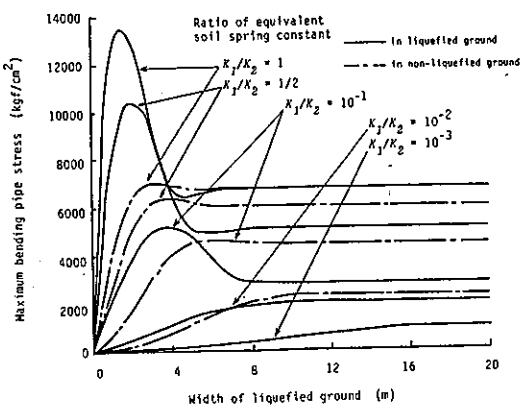

Fig. 4 Relationship between maximum bending pipe stress due to subsidence of liquefied ground and width of liquefied zone.

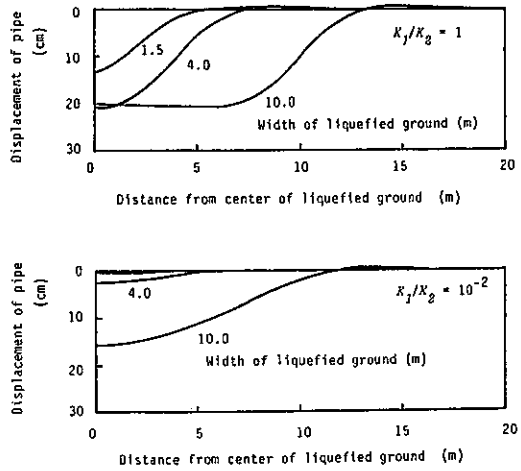

Fig. 5 Distribution of pipe displacement due to subsidence.

equivalent soil spring constant, the relative displacement between the ground and pipe is observed. The maximum displacement of the pipe decreases because rigidity of the pipe dominates that of the ground. In case 1, the location where the maximum bending stress occurs coincides with the pipe located at the center of the liquefied zone ; however, for greater width of the liquefied ground or higher ratio of the equivalent soil spring constant, the location is nearer the boundary between the liquefied and non-liquefied ground.

Table 2 Physical properties of steel pipe.

Outer diameter	(mm)	406.4
Thickness	(mm)	6.0
Young's modulus	(kgf/cm²)	2.1×10^6
Specific gravity		7.85

(1kgf/cm²=98kPa)

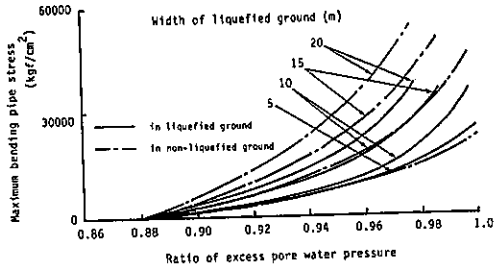

Fig. 6 Relationship between maximum bending pipe stress due to buoyancy effects induced by liquefaction and excess pore water pressure ratio.

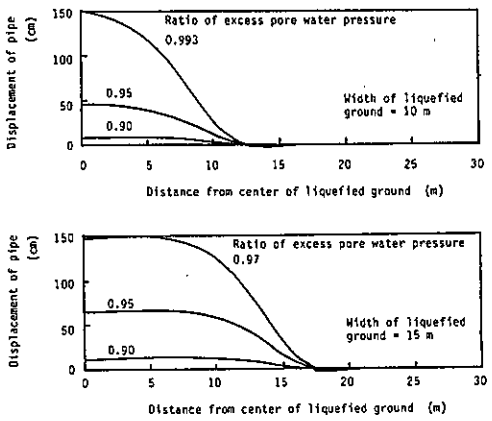

Fig. 7 Distribution of pipe displacement due to buoyancy effects.

In case 2, the buoyancy effects of the pipelines during liquefaction are estimated by using the method described by Kitaura and Miyajima[6]. Fig. 6 shows the relationship between the maximum bending pipe stress due to buoyancy effects induced by liquefaction and the excess pore water pressure. Fig. 7 illustrates the relationship between the displacement of the pipe and the width of the liquefied ground. In this study, the equivalent soil spring constant of the liquefied soil is estimated by the empirical equation proposed by Yoshida and Uematsu[7]. It was noted that the pipe reached the ground surface in the area where the width of liquefied ground exceeded

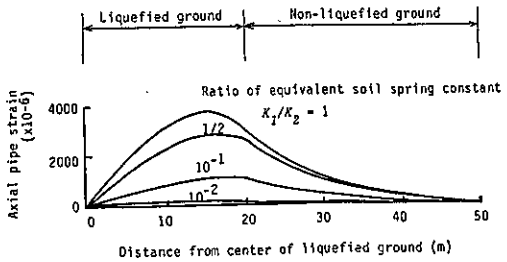

Fig. 8 Distribution of axial pipe strain in relation to ratio of equivalent soil spring constant.

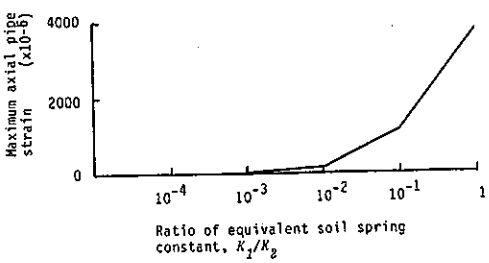

Fig. 9 Relationship between maximum axial pipe strain and ratio of equivalent soil spring constant.

10m as shown in Fig. 7. Therefore, the maximum bending pipe stresses disappear for great width and high excess pore water pressure in Fig. 6. It is evident from Fig. 6 that the greater the width of the liquefied ground is, the higher the maximum bending stresses are, that is, the greater the probability of failure of the pipe due to buoyancy effects. It is also interesting to note that the maximum bending pipe stresses occurred in the non-liquefied ground in case of great width of the liquefied ground. In these analyses, it is assumed that the duration of the liquefaction process is lengthy enough to allow the occurrence of pipe deformation. However, since the duration of liquefaction induced by a real earthquake depends on the local soil conditions, the above may actually not be the cases in reality. Therefore, these results may be overestimated. In order to evaluate the pipeline response due to buoyancy effects more precisely, the method proposed by Kitaura et al.[8] is preferable.

In case 3, the distribution of the axial pipe strain is shown in Fig. 8, in relation to the ratio of the equivalent soil spring constant K_1/K_2. Fig. 9 illustrates the relationship between the maximum axial pipe strain and the ratio of the equivalent soil spring constant. The conditions for the ground and the magnitude of an earthquake used in these analyses are summarized in Table 3. It is evident from these figures that the maximum axial strains decrease and the location where the maximum strains occurs approaches the boundary of the ground with a decrease in the ratio. During liquefaction processes, not only the equivalent soil spring constant varies but also longitudinal wave velocity c varies. Therefore, the longitudinal wave velocity is

Table 3 Conditions of ground and magnitude of earthquake.

Longitudinal wave velocity c	170(m/s)
Period of shaking T	0.5(s)
Acceleration in superficial layer α	200(gal)
Displacement amplitude of non-liquefied superficial layer	$U_{s_0}=(T/2\pi)^2\alpha$

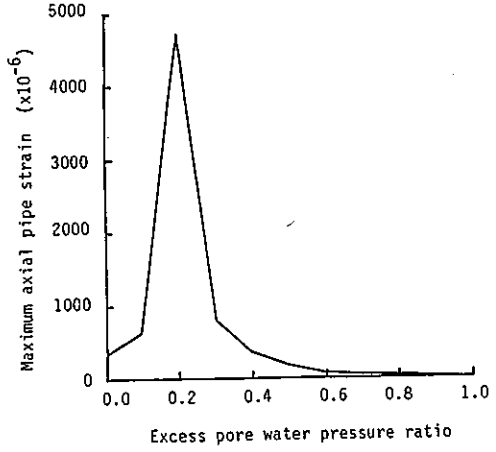

Fig. 11 Relationship between maximum axial pipe strain and excess pore water pressure ratio.

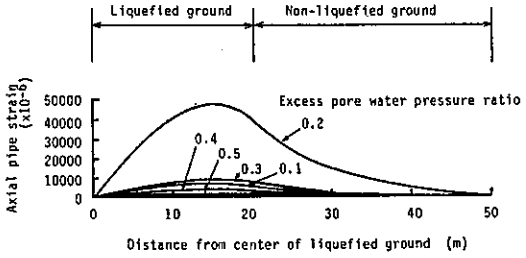

Fig. 10 Distribution of axial pipe strain in relation to excess pore water pressure.

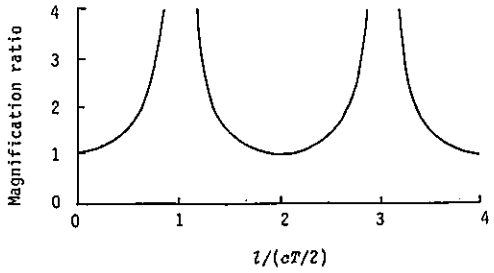

Fig. 12 Magnification ratio of response displacement in superficial layer.

assumed to be proportional to the fourth root of $(1-r)$, where r is the excess pore water pressure ratio because the longitudinal wave velocity is proportional to the square root of Young's modulus of soil, and the shear modulus of the soil is proportional to the square root of $(1-r)$. Moreover, Young's modulus is proportional to the shear modulus of the soil. Fig. 10 shows the distribution of the axial pipe strain in relation to the excess pore water pressure ratio. Fig. 11 illustrates the relationship between the maximum axial pipe strain and the excess pore water pressure ratio. Excess pore water pressure higher than 0.9 is not included in this analysis because the longitudinal wave cannot be transmitted in such soft ground. It is evident from these figures that the maximum axial pipe strain occurs at the liquefied ground near the boundary between the liquefied and non-liquefied ground. The maximum axial pipe strain corresponding to the value of 0.2 of excess pore water pressure ratio is markedly great. This can be explained as follows : Fig 12 shows the magnification ratio of response displacement in a superficial layer. In this analysis, $1/(cT/2)$ is less than 1.0 ; therefore, the magnification ratio increases sharply with an increase in $1/(cT/2)$, i.e. with a decrease in c. However, in this case the magnification ratio decreases because $1/(cT/2)$ is greater than 1.0. Effects of the resonance of the liquefied ground are great when excess pore water pressure ratio is equal to 0.2. Furthermore, Fig. 12 suggests that care should also be taken in evaluating the resonance of the liquefied ground for greater width of liquefied ground than that in this analysis. The above results obtained by mathematical analyses suggest that the probability of failure is high at the boundary between the liquefied and non-liquefied ground for each cause of pipe failure. These findings agree with the experimental results presented in Ref. 9.

4. Conclusions

Response characteristics of pipelines located through both liquefied and non-liquefied ground were clarified based on mathematical analysis. The following can be concluded :

(1) One of the response characteristics of pipelines subjected to subsidence of ground is that the smaller the degree of liquefaction in the superficial ground, the greater the maximum bending pipe stresses. Moreover, the higher bending pipe stress occurs in areas of smaller width of the liquefied ground.

(2) The effects of buoyancy on pipe response are great in areas of great width of the liquefied ground and a high degree of liquefaction in the superficial ground.

(3) Resonance of the superficial layer of ground has great influence on the axial pipe strains during liquefaction processes. This suggests that great consideration should be given to vibration-induced strains during liquefaction.

Nomenclature

A : cross-sectional area of the pipe

c : longitudinal wave velocity $=\sqrt{E_s/\rho}$

E : Young's modulus of the pipe material

E_s : Young's modulus of soil
F : a force caused by the buoyancy effect
I : area moment of inertia of the pipe
K_v, K_u : equivalent spring constants for the longitudinal and transverse motions
L : pipe length
l : width of the liquefied zone
T : period of shaking
U, V : displacements in the ground
u, v : longitudinal and transverse displacements in the pipeline
u_{s_0} : displacement amplitude in non-liquefied superficial layer

Greek letters

β^4 : $K_v/4EI$
λ^2 : K_u/EA
ρ : soil density

Subscripts

1 : liquefied ground
2 : non-liquefied ground

References

1) Kitaura, M. and Miyajima, M. : Assessment of Safety of Pipelines Subjected to Soil Liquefaction, Preliminary Report of IABSE Symposium TOKYO 1986, Vol. 51, pp. 133-140, 1986.
2) Kitaura, M and Miyajima, M. : Response Simulation of Buried Pipeline During Soil Liquefaction, Memoirs of the Faculty of Technology, Kanazawa University, Vol. 17, No. 1, pp. 11-18, 1984.
3) Nishio, N., Tsukamoto, K. and Hamura, A. : Model Experiment on the Seismic Behavior of Buried Pipeline in Partially Liquefied Ground, Proceedings of JSCE, No. 380, pp. 449-458, 1987 (in Japanese).
4) Yoshimi, Y., Kuwabara, F. and Tokimatsu, K. : One-dimensional Volume Change Characteristics of Sands under Very Low Confining Stresses, Soils and Foundations, JSSMFE, Vol. 15, No. 3, pp. 51-60, 1975.
5) Lee, K. L. and Albaisa, A. : Earthquake Induced Settlements in Saturated Sands, Proceedings of ASCE, Vol. 100, No. GT4, pp. 387-406, 1974.
6) Kitaura, M. and Miyajima, M. : Dynamic Behavior of Buried Model Pipe During Incomplete Liquefaction, Journal of Structural Engineering, JSCE, Vol. 31A, pp. 421-426, 1985 (in Japanese).
7) Yoshida, T. and Uematsu, M. : Dynamic Behavior of a Pile in Liquefaction Sand, Proceedings. of the 5th Japan Earthquake Engineering Symposium-1978, pp. 657-663, 1978 (in Japanese).
8) Kitaura, M., Miyajima, M. and Suzuki, H. : Response Analysis of Buried Pipelines Considering Rise of Ground Water Table in Liquefaction Processes, Proceedings of JSCE, No. 380/I-7, pp. 173-180, 1987.
9) Kitaura, M. and Miyajima, M. : Dynamic Behaviour of a Model Pipe Fixed at One End During Liquefaction, Proceedings of JSCE, No. 336, pp. 31-38, 1983 (in Japanese).

(Received October 29, 1988)